Liquid Crystals
Publication details, including instructions for authors and subscription information:
http://www.informaworld.com/smpp/title~content=t713926090

Polymer network structure and electro-optic performance of polymer stabilized cholesteric textures II. The effect of UV curing conditions

I. Dierking; L. L. Kosbar; A. C. Lowe; G. A. Held

To cite this Article Dierking, I. , Kosbar, L. L. , Lowe, A. C. and Held, G. A.(1998) 'Polymer network structure and electro-optic performance of polymer stabilized cholesteric textures II. The effect of UV curing conditions', Liquid Crystals, 24: 3, 397 — 406
To link to this Article: DOI: 10.1080/026782998207217
URL: http://dx.doi.org/10.1080/026782998207217

Liquid Crystals, 1998, Vol. 24, No. 3, 397–406

Polymer network structure and electro-optic performance of polymer stabilized cholesteric textures
II. The effect of UV curing conditions

by I. DIERKING†, L. L. KOSBAR, A. C. LOWE and G. A. HELD*
IBM T.J. Watson Research Center, P.O. Box 218, Yorktown Heights, NY 10598, USA

(*Received 6 August 1997; accepted 8 September 1997*)

The effect of UV curing intensity and curing time on the electro-optic behaviour and network morphology of reverse mode polymer stabilized cholesteric textures (PSCTs) has been studied. Scanning electron micrographs indicate that increasing the curing intensity generally results in a more open polymer network characterized by a larger average void size, while the morphology of the individual strands remains largely unchanged. In addition, as the polymerization process proceeds, voids within the network are observed to decrease in size. PSCTs with sufficiently large network voids exhibit a two-stage switching behaviour consistent with a model in which the cholesteric liquid crystal is divided between two distinct environments—one in which the liquid crystal is strongly dominated by the polymer network, the other in which a bulk-like behaviour, comparable to the unstabilized cholesteric material, is observed.

1. Introduction

In this second part [1] of our study on the effects of processing conditions on the electro-optic performance and polymer morphology of *reverse mode* polymer stabilized cholesteric textures (PSCTs) [2, 3], we address the dependence of these systems on varying UV curing conditions—both intensity and total dose. We find that increasing the curing intensity increases the average void size within the network and that this changes the electro-optic properties of the system in a manner consistent with a model in which the polymer is divided between two distinct environments—one 'bulk-like', the other strongly dominated by the polymer network [4]. In particular, as the curing intensity is increased, we observe a cross-over from one- to two-stage switching similar to that observed for decreasing polymer concentration and increasing curing temperature. However, as with variations in curing temperature, changing the curing intensity is found to have little effect on the structure of individual polymer strands.

When the UV intensity is fixed and the total curing time (and thus the total UV dose) is decreased, a structure with increasingly large voids is observed. During the early stages of the polymerization process, a low density network which contains both polymer beads and strands is observed. As the curing time is increased, the polymer network evolves into a denser network consisting entirely of highly interconnected strands. As the density of the network increases, a cross-over from two- to one-stage switching is observed which is again consistent with the two environment model for the polymer stabilized liquid crystal material.

2. Experimental

The nematic matrix used in this study was the mixture E48 (Merck Industries) doped with 0·5 wt % of the chiral agent R1011 (Merck Industries) to produce an induced cholesteric phase with a pitch of 10 μm. The mesogenic diacrylate monomer RM206‡ was dissolved in the chiral nematic liquid crystal at 6 wt %. A small amount (2 wt %) of benzoin methyl ether (BME) was added to the monomer to act as a photoinitiator. The liquid crystal–monomer solutions were vacuum filled into 15-μm-thick cells with low pretilt, anti-parallel rubbed polyimide alignment layers, where the cell thickness was controlled by a dispersion of cylindrical spacer beads. The cells were sealed and UV irradiated with the liquid crystal in the planar orientation. Thus, the resulting polymer network structure was expected to follow the local helical order of the liquid crystal. The

---

† Present address: Liquid Crystal Group, Physics Department, Chalmers University of Technology, S-41296 Göteborg, Sweden.

*Author for correspondence.

‡ The exact structure of RM206 is proprietary to Merck Industries.

UV source was a mercury lamp attenuated with Pyrex glass such that the strongest UV emission was at 365 nm. Variations in UV intensity between 0·01 and 5·4 mW cm^{-2} were carried out at a fixed exposure time of 5·5 h. Variations in exposure time were made at a fixed intensity of 0·5 mW cm^{-2}.

The diffuse reflectivity (fraction of back scattered light) and the diffuse transmittance (fraction of forward scattered light) were measured on an absolute scale using an integrating sphere (Oriel Instruments). Texture transitions were induced by a sine wave voltage of frequency 2–5 kHz at variable amplitude, and the sample was illuminated with a 633 nm HeNe laser. Depending on the detection method employed, either the static or dynamic response of the cell was measured [4]. For dynamic measurements, the electric field amplitude was chosen to ensure a saturated switching process and response times were evaluated for a 10–90% change of light intensity. Except as noted (figure 8), the samples showed no significant hysteresis.

Scanning electron microscope investigations (Hitachi S-800 SEM) of the polymer networks were carried out following removal of the liquid crystal from the samples. Sample preparation for the SEM studies was carried out according to a procedure which evidence suggests to be non-destructive [1].

3. Results and discussion

3.1. *UV intensity variation*

The experimentally determined diffuse reflectivity and transmittance of 6 wt % RM206 PSCT cells, measured for different UV curing intensities, are shown in figure 1 (*a*) and 1 (*b*), respectively. Only those RM206 samples which were cured at intensities above approximately 1 mW cm^{-2} exhibit two-stage switching in the diffuse reflectivity and, even in several of these cases, the two stages are not observable in the reflectivity versus voltage data. The two reorientation processes in RM206 samples cured at high intensities (as well as the single-stage reorientation process in samples cured at lower intensities) can, however, be observed clearly in time resolved measurements of the diffuse reflectivity (figure 2). When the electric field is removed at $t = 50$ ms, the diffuse reflectivity reveals the dynamics of the transition from the focal-conic to the planar state. For the sample cured at 5·4 mW cm^{-2}, a fast reorientation is followed by a second, much slower process, whereas for the sample cured at 0·05 mW cm^{-2}, only a single, fast reorientation process can be observed. All of the diffuse transmittance data exhibit only single-stage switching, as previously observed for variations in both polymer concentration and curing temperature [1, 4]. Generally, we observe a decrease in the maximum diffuse reflectivity with increasing curing intensity [figure 3 (*a*)] as well as an increase in the diffuse transmittance [figure 3 (*b*)]. Neither of these trends, however, is statistically significant. Similarly, the threshold voltages for the onset of diffuse reflectivity and transmittance appear to decrease slightly with increasing curing intensity (figure 4).

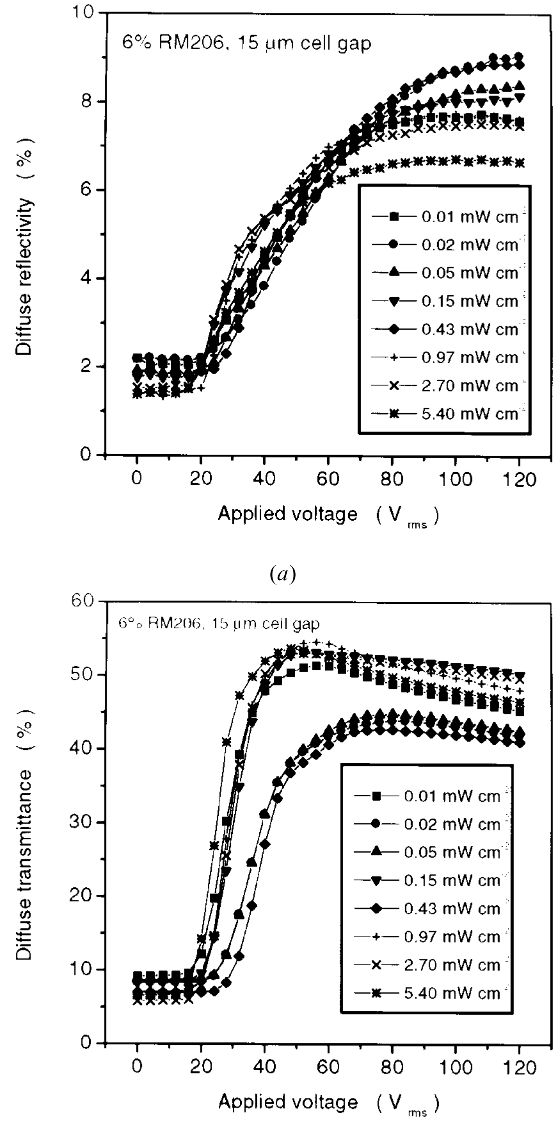

(*a*)

(*b*)

Figure 1. (*a*) Diffuse reflectivity and (*b*) diffuse transmittance as a function of applied voltage for 6 wt % RM206 polymer stabilized samples prepared at various curing intensities.

PSCT cells have two distinct dynamic responses—one for the transition from the planar to the focal-conic state (the rise time), the other for the switching from the field induced, scattering focal-conic state back to the planar, non-scattering texture at zero field (the decay time). The former reorientation process is dependent on the applied

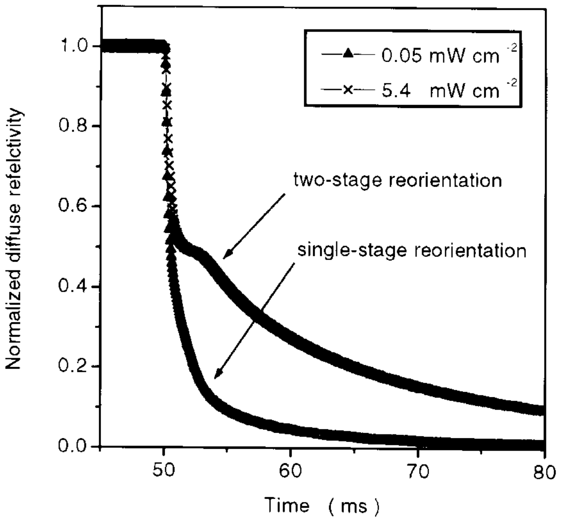

Figure 2. Dynamic response of the diffuse reflectivity of 6 wt % RM206 samples. These data show the reorientation from the focal-conic to the planar state following the removal of the applied field at $t=50$ ms. For high curing intensities (5·4 mW cm^{-2}) a two-stage switching is observed, whereas only a single-stage reorientation is observed for low curing intensities (0·05 mW cm^{-2}).

electric field amplitude, as dielectric interactions are driving this transition. Thus, rise times can be compared only if the same voltage can be applied to all of the samples. For this reason, all dynamic response measurements were taken with driving voltages of 120 V rms. The relaxation process following removal of the applied field is basically governed by elastic forces between the polymer network and the liquid crystal; thus the decay times can, to first approximation, be considered as electric field independent. Rise times of the diffuse reflectivity and diffuse transmittance as a function of UV curing intensity are shown in figure 5 (*a*). These data yield information on residues of oligomers or short chain polymer fractions, as these would drastically increase the viscosity of the systems, and thus increase the rise times. The absence of a significant change in rise times as the UV curing intensity is varied over three orders of magnitude suggests that all of the monomer material is incorporated into the polymer network. The observed decay times, however, do increase strongly with increasing curing intensity above approximately 1 mW cm^{-2} [figure 5 (*b*)]. This suggests that an increased curing intensity results in a greater fraction of the liquid crystal being in regions of low polymer density and, thus, the polymer network playing a less dominant role in the reorientation process.

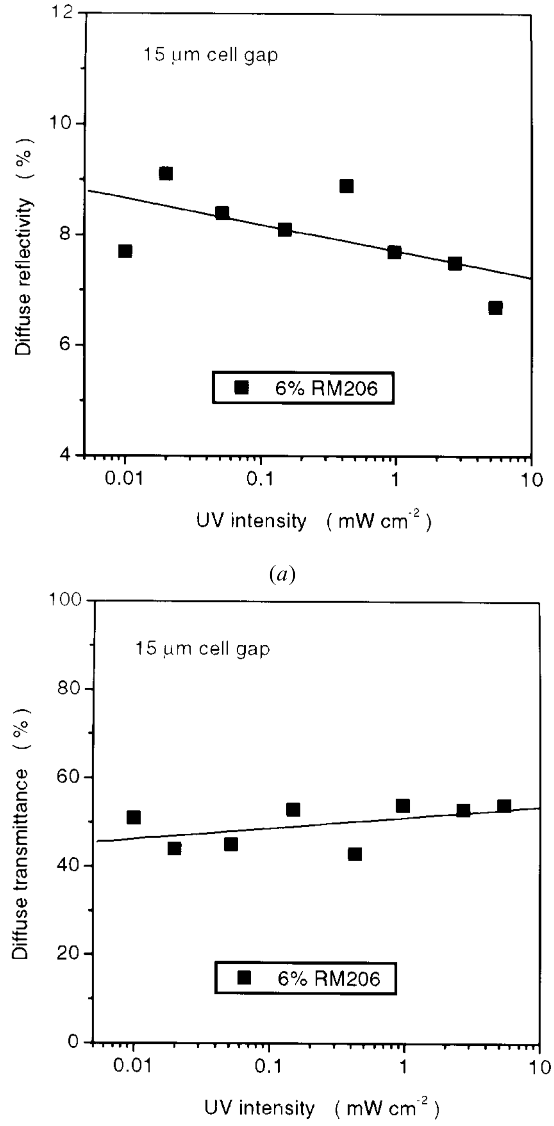

(*a*)

(*b*)

Figure 3. Dependence of the maximum observed (*a*) diffuse reflectivity and (*b*) diffuse transmittance on curing intensity for 6 wt % RM206 polymer networks.

The trends in the electro-optical data which are observed with increasing curing intensity are similar to those observed when either the curing temperature of a PSCT system is increased or the concentration of the polymer network is decreased. That is, as the curing intensity is increased the diffuse reflectivity decreases, the diffuse trnasmittance increases, and the threshold voltages for both diffuse reflectivity and transmittance decrease. These same trends are all observed for decreasing polymer content [4]. Further, as the curing intensity of RM206 PSCTs is increased, a transition from one- to two-stage switching, similar to that observed for decreasing RM206 content or increased curing temperature, is observed. In those cases it was shown that the lower polymer concentrations [4] and increased curing

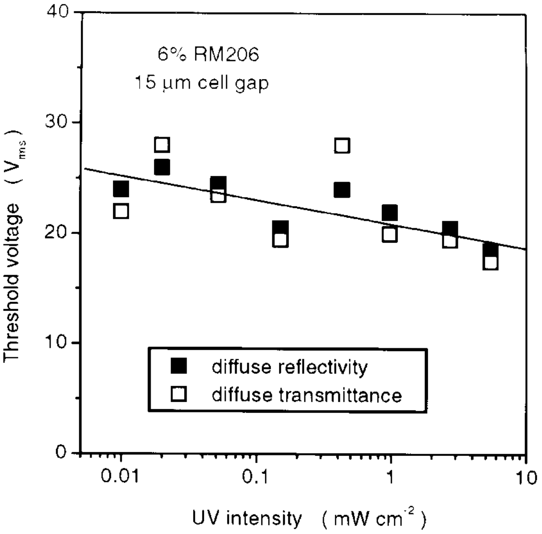

Figure 4. Dependence of the threshold voltages of the diffuse reflectivity (■) and diffuse transmittance (□) of the planar to focal-conic texture transition on curing intensity for 6 wt % RM206 polymer networks.

temperatures [1] both resulted in larger voids within the polymer network. This, in turn, resulted in larger regions of 'bulk-like' liquid crystal material. It was argued that the presence of both 'bulk-like' and polymer dominated regions of liquid crystal material resulted in the observation of two-stage switching. The present data are consistent with this model provided that increasing the curing intensity of a PSCT cell results in larger voids within the polymer network.

Figure 6 (*a*)–(*d*) shows SEM images of 6 wt % RM206 PSCT polymer networks which have been UV cured at 0·05, 0·15, 2·7 and 5·4 mW cm^{-2}, respectively. In these images, one observes a decrease in strand density with increasing curing intensity. Most notably, the images taken from PSCT cells which exhibited two-stage switching [figure 6 (*c*) and (*d*)] reveal a more open network of strands (as well as larger voids) than do those taken from cells which show only single stage switching [figure 6 (*a*) and (*b*)]. These images are consistent with a model that associates the long timescale reorientation process with bulk-like liquid crystal regions, while the high threshold, fast decay time process is associated with regions which are strongly influenced by the polymer network. Based on estimates from the 6 wt % RM206 SEM data, we find that an average void size of 0·4–0·5 μm is observed near the transition from one- to two-stage switching. It is noteworthy that this same average void size is also observed at the cross-over between one- and two-stage switching when either the polymer concentration or the curing temperature is varied [1, 4].

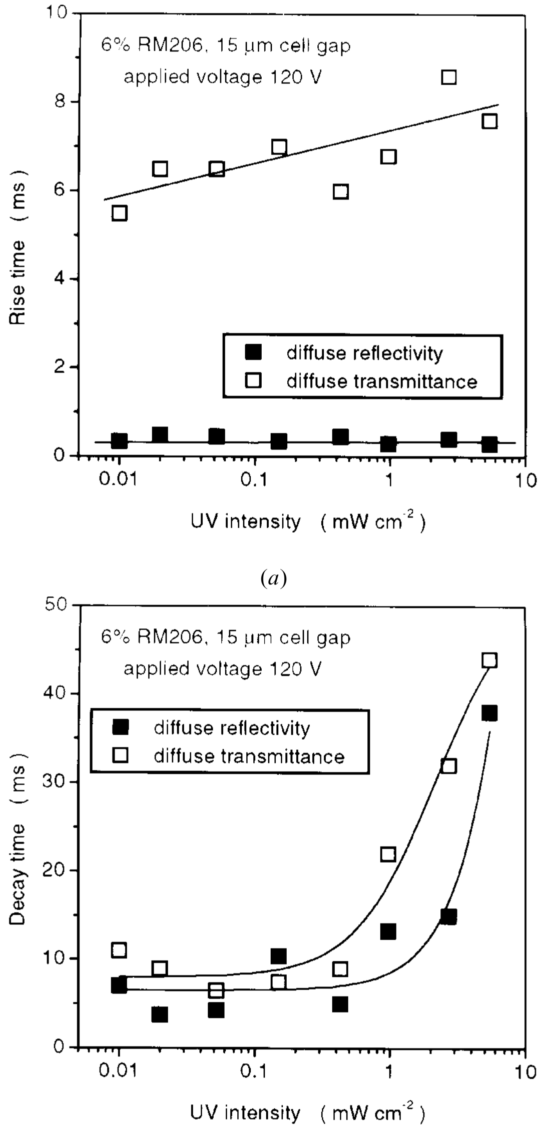

(*a*)

(*b*)

Figure 5. Dependence of the (*a*) rise times and (*b*) decay times of the diffuse reflectivity (■) and diffuse transmittance (□) on curing intensity for 6 wt % RM206 polymer networks.

We find that the helical structure of the cholesteric is more clearly transferred to the polymer network in cells which exhibit only single stage switching. In figure 7 (*a*), an SEM image of a 6 wt % RM206 polymer network cured at 0·05 mW cm^{-2}, the helical structure is clearly visible, whereas in figure 7 (*b*), the image of a network cured at 5·4 mW cm^{-2}, it is not. We note that even in networks where this helical structure is not observable with SEM it is possible to resolve a partial helical order *in situ* using confocal microscopy [5]. While there is no obvious correlation between helical order and the

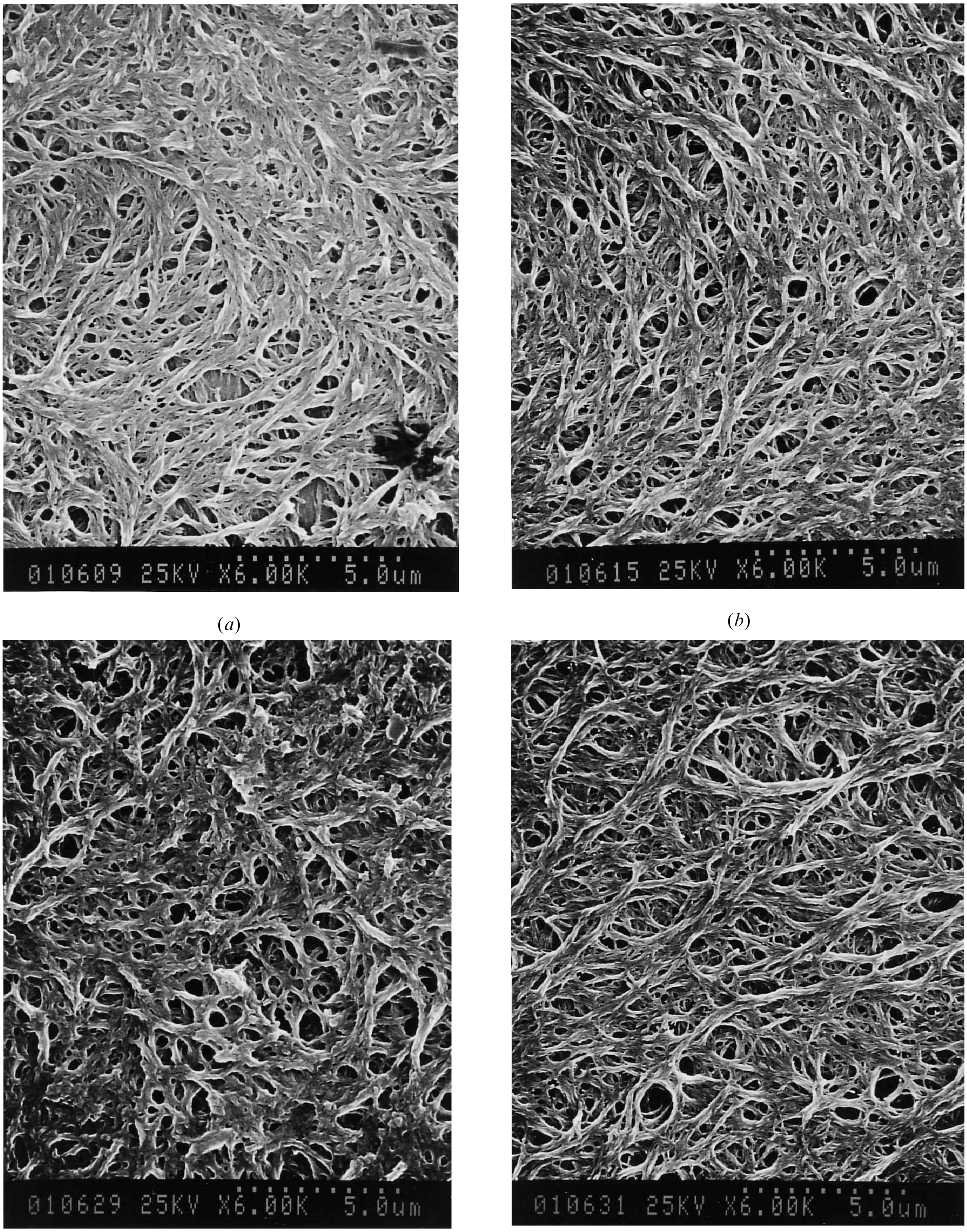

(*a*) (*b*)

(*c*) (*d*)

Figure 6. SEM photographs of the polymer network structure of 6 wt % RM206 formed at different curing intensities. (*a*) 0·05, (*b*) 0·15, (*c*) 2·7 and (*d*) 5·4 mW cm^{-2}. The dimensions of the regions shown are $14{\cdot}4 \times 17{\cdot}2\,\mu m^2$.

electro-optic properties of the PSCT cell, it is certainly reasonable that a polymer network, which on average closely followed the liquid crystalline order during polymerization, would have larger elastic interactions with the liquid crystal than would one which polymerized into a randomly oriented polymer network.

For all curing intensities, the RM206 networks consist of a tight network of fine, highly interconnected polymer fibres. That is, the curing intensity during the polymerization process does not strongly affect the morphology of the individual polymer strands, it simply affects the size of the voids within the polymer network. Further, it remains surprising that changing the curing intensity by a factor of 500 has such a small effect on both the network morphology and the electro-optic behaviour of the PSCT cells.

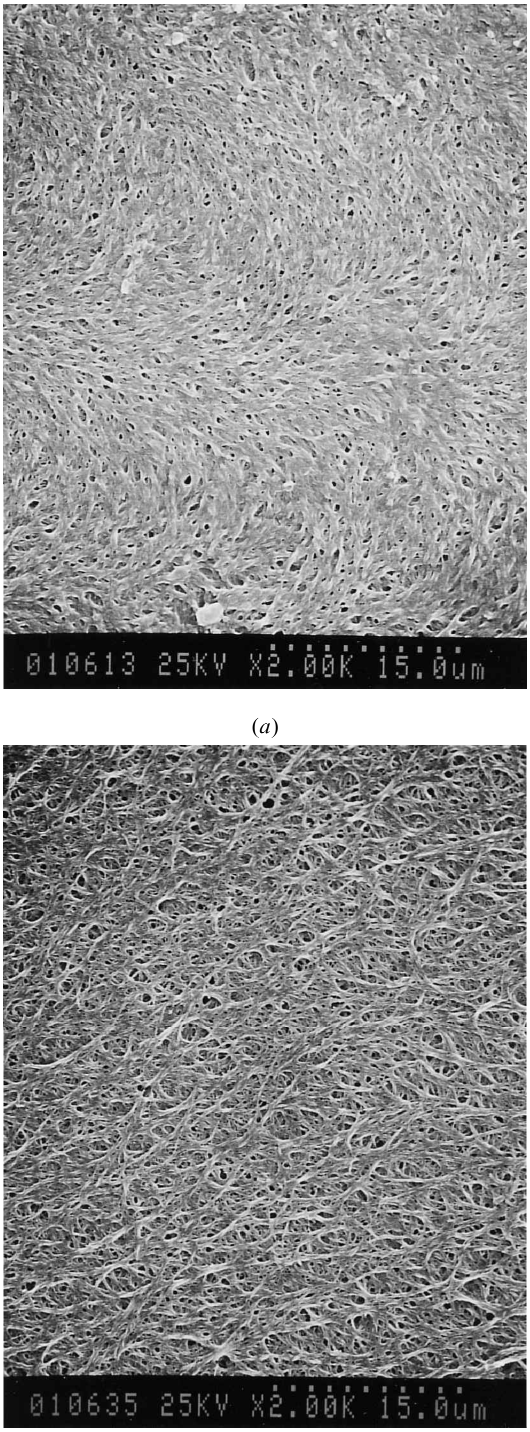

(*a*)

(*b*)

Figure 7. Large area SEM photographs of the polymer network structure of 6 wt % RM206 formed at different curing intensities. (*a*) 0·05 and (*b*) 5·4 mW cm^{-2}. The dimensions of the regions shown are $43{\cdot}2 \times 51{\cdot}6\,\mu m^2$. The helical order of the cholesteric liquid crystal is clearly observable only in (*a*).

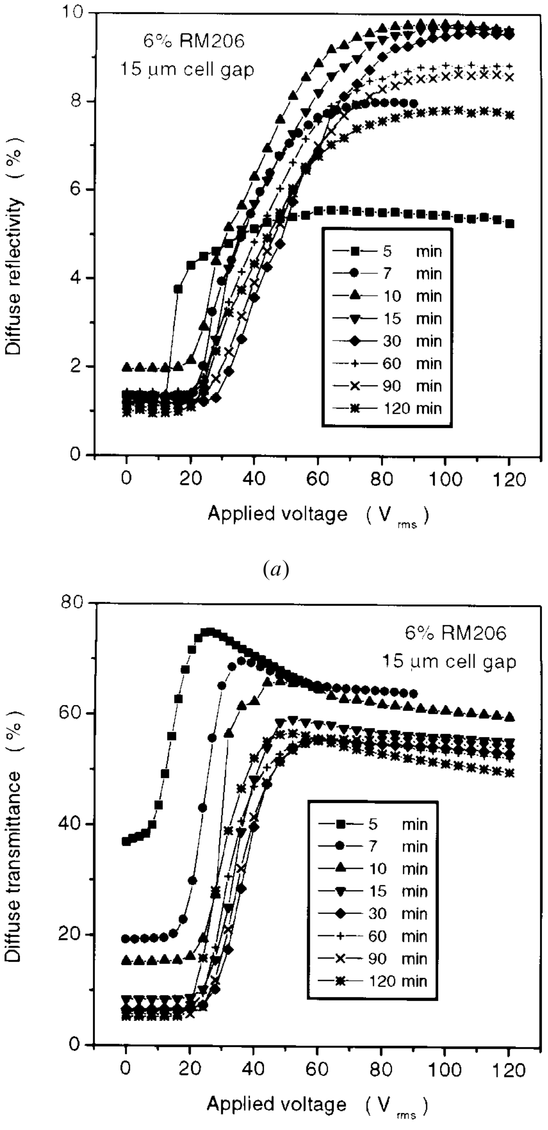

(*a*)

(*b*)

Figure 8. (*a*) Diffuse reflectivity and (*b*) diffuse transmittance as a function of applied voltage for 6 wt % RM206 polymer stabilized samples cured for various time periods. The reflectivity data for the samples cured for 5 and 7 min were not reversible—following removal of the applied voltage these samples remained in partially scattering focal-conic states. This accounts for the anomalously high diffuse transmittance observed for these samples at 0 volts.

3.2. *UV dose variation*

The experimentally determined diffuse reflectivity and transmittance of 6 wt % RM206 PSCT cells, measured for different UV curing times at a fixed curing intensity of 0·5 mW cm^{-2}, are shown in figure 8 (*a*) and (*b*), respectively. Only those RM206 samples which were cured for less than 30 min exhibit two-stage switching in the diffuse reflectivity. As with variations in curing intensity, the two-stage switching is not always readily observable in the reflectivity versus voltage data. However, the two reorientation processes for short curing times (as well as the single-stage reorientation process in samples cured for longer periods) can be observed clearly in time resolved measurements of the diffuse reflectivity (figure 9) where the sample cured for 5 min clearly exhibits two reorientation processes. As with earlier variations in processing conditions, all of the diffuse transmittance data exhibit only single-stage switching. We observe a sharp increase in the maximum diffuse reflectivity as the curing time is increased to 30 min, whereas after 30 min no significant changes occur [figure 10 (*a*)]. Likewise, during the initial 30 min we observe sharp decreases in both the diffuse transmittance [figure 10 (*b*)] and the threshold voltages [figure 11].

We observe a significant increase in the rise time [figure 12 (*a*)] and decrease in the decay time [figure 12 (*b*)] as the curing time is increased from 4 to 30 min. It is possible that the initial increase in rise times results from the formation of oligomers and short polymer chains which increase the viscosity of the liquid crystal. However, as the rise times do not fall with further polymerization, our data suggest that the completed polymer network does in fact slow the switching rate from the planar into the focal-conic texture, even in the absence of oligomers within the liquid crystal. That is, it is possible that the increase in rise time with increased curing time results from an increased anchoring energy between the liquid crystal and the polymer network. Given that the total liquid crystal/polymer interfacial area is increasing with increased curing time (as the total density of the polymer network increases, figure 13), such an increase in liquid crystal/polymer interfacial energy seems quite reasonable. Further, an increase in

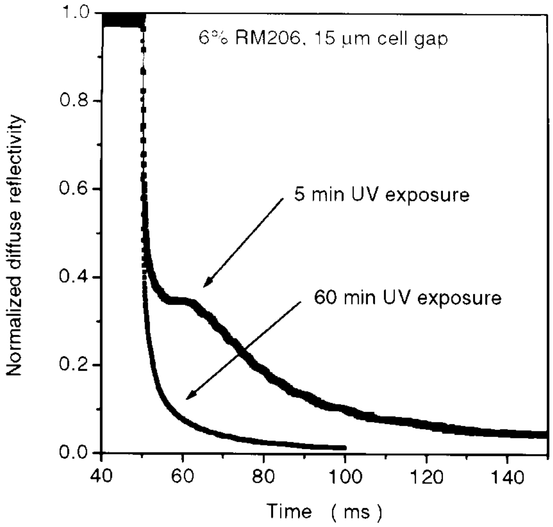

Figure 9. Dynamic response of the diffuse reflectivity of 6 wt % RM206 samples following the removal of the applied field at $t=50$ ms. For short curing times (5 min) a two-stage switching is observed, whereas only a single stage reorientation is observed for longer curing times (60 min).

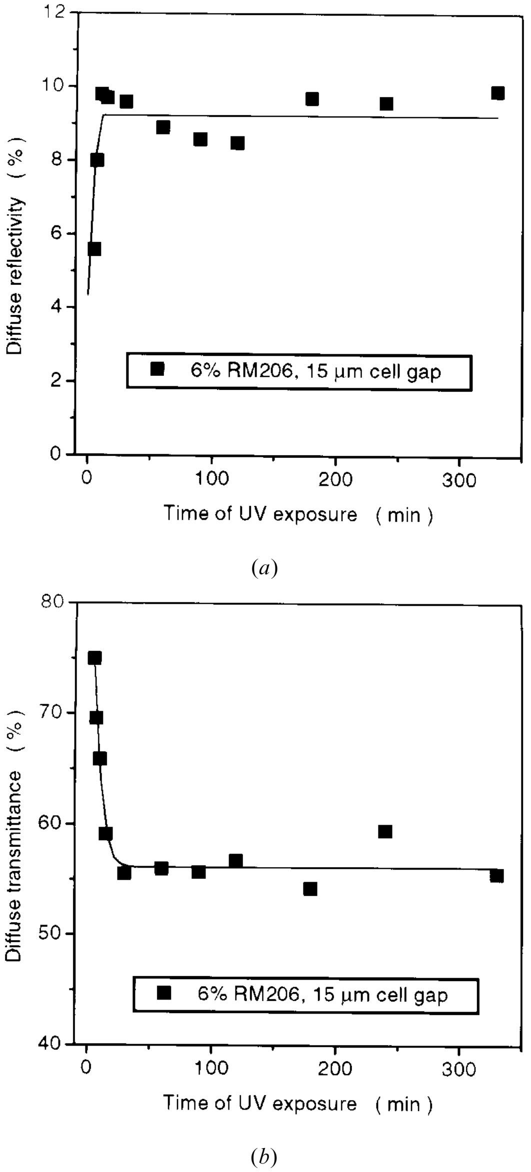

(*a*)

(*b*)

Figure 10. Dependence of the maximum observed (*a*) diffuse reflectivity and (*b*) diffuse transmittance on curing time for 6 wt % RM206 polymer networks.

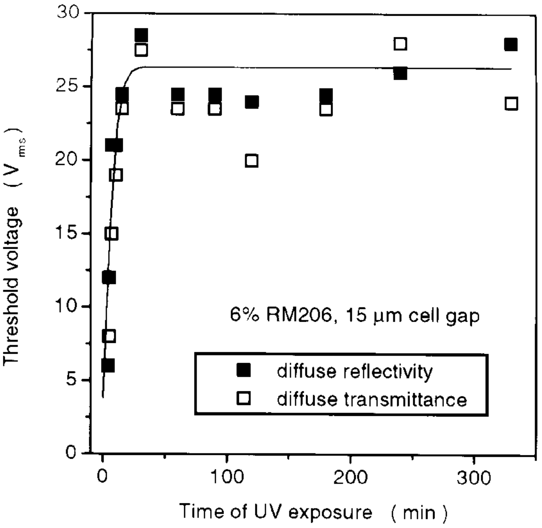

Figure 11. Dependence of the threshold voltages of the diffuse reflectivity (■) and diffuse transmittance (□) of the planar to focal-conic texture transition on curing time for 6 wt % RM206.

interfacial energy would also be consistent with the observed decrease in decay times.

All of the electro-optical data presented above show trends with increasing curing time similar to those observed for decreasing curing temperature, decreasing curing intensity, and increasing polymer concentration. That is, we observe decreasing diffuse transmittance, increasing diffuse reflectivity, increasing threshold voltages, and decreasing decay times as the curing time is increased towards 30 min. Further, as the curing time is decreased, a transition from one- to two-stage switching, similar to that observed for decreasing RM206 content, is observed. All of these data suggest that as the curing time is increased, the average void size within the polymer network decreases.

Figure 13 (*a*)–(*d*) shows SEM images of 6 wt % RM206 PSCT polymer networks which have been UV cured at 0·5 mW cm^{-2} for 4, 5, 10 and 30 min, respectively. For curing times longer than 30 min no further change in the network structure can be detected with SEM. From these images it is clear that the mean void size within these networks does indeed decrease with increased curing time. Further, these figures provide a clear picture of the various stages of the polymerization of RM206 in a cholesteric environment. After 4 min [figure 13 (*a*)] only a small fraction of the polymerization has occurred, yet a network which permeates the cell is already present. This network includes fine strands, plate-like regions of polymer, and small beads of polymer attached to the network. At 5 min [figure 13 (*b*)], a much denser network has formed. At this point the network is composed primarily of strands, although some beads remain. After

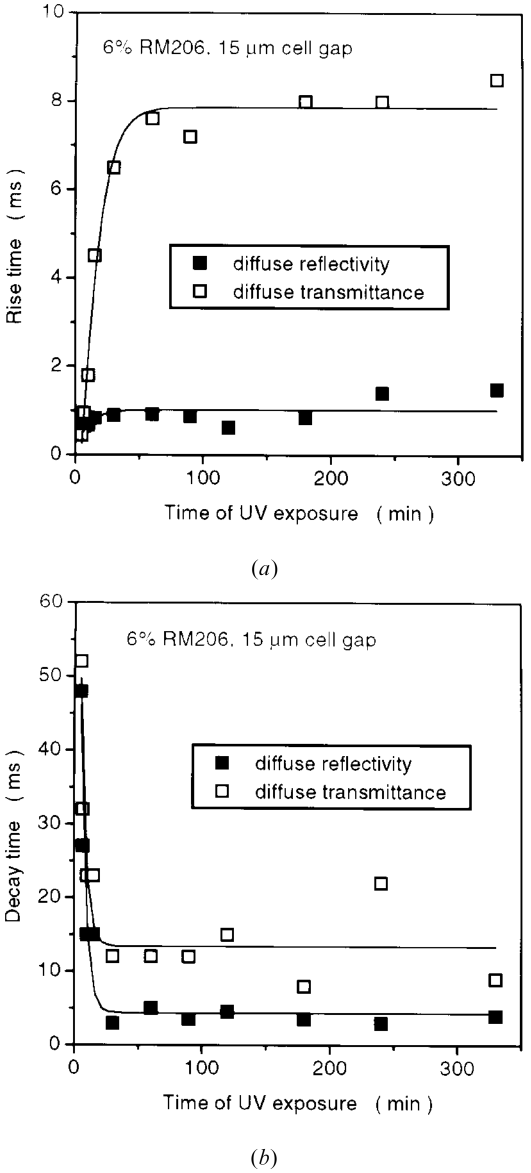

(*a*)

(*b*)

Figure 12. Dependence of the (*a*) rise times and (*b*) decay times of the diffuse reflectivity (■) and diffuse transmittance (□) on curing time for 6 wt % RM206 polymer networks.

10 min of polymerization [figure 13 (*c*)] the network has become denser still, while the beads are no longer discernible. From these data alone it is not possible to determine the mechanism by which the beads disappear and the strands become more uniform. Possibilities include the incorporation of additional monomer onto the existing network as well as further crosslinking and the expulsion of liquid crystal from within the beads. We note that a similar evolution from bead-like to fibrous morphology has been observed with increasing UV dose during polymerization in nematic liquid crystals [6]. As with variations of the curing intensity, we

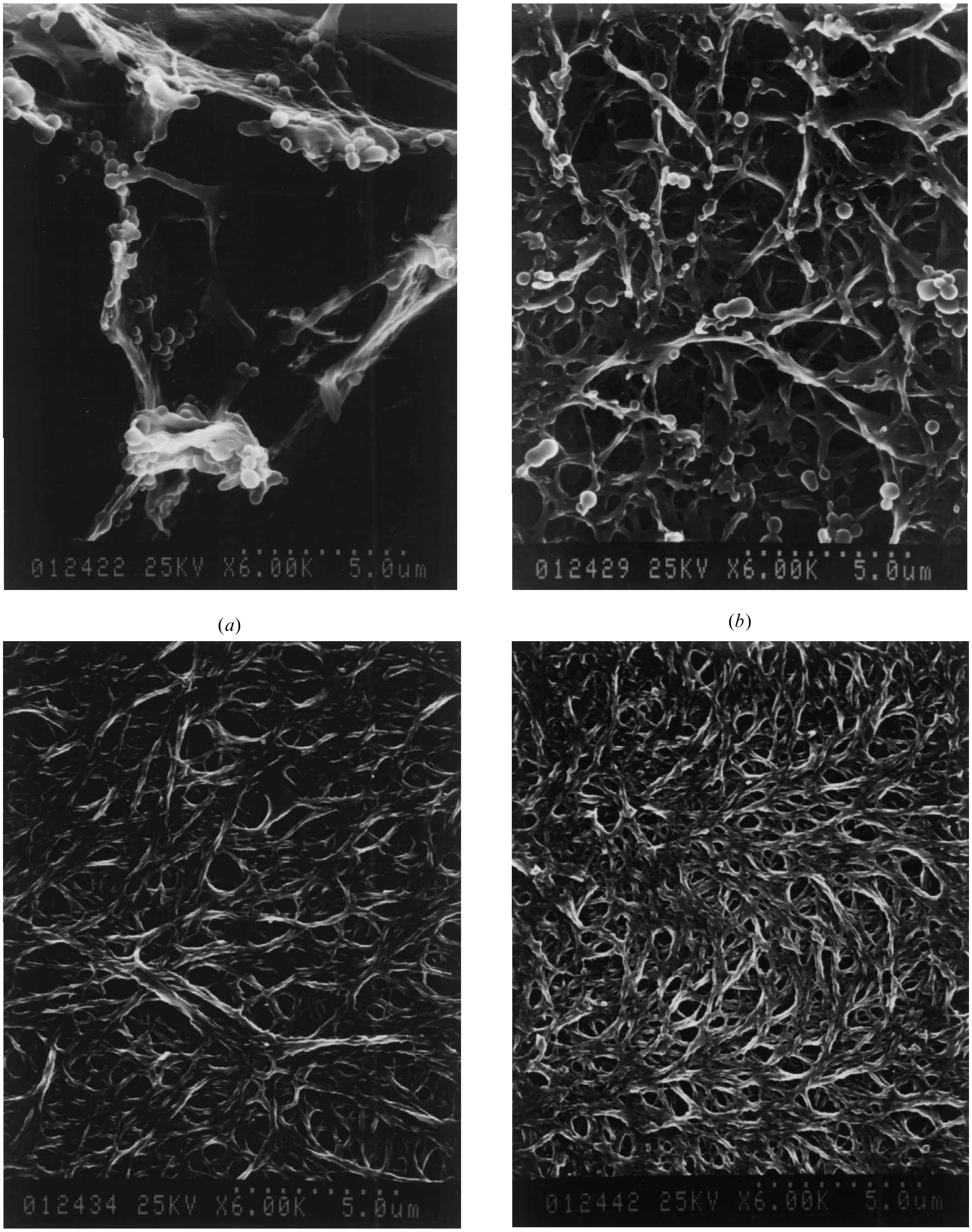

(*a*) (*b*)

(*c*) (*d*)

Figure 13. SEM photographs of the polymer network structure of 6 wt % RM206 formed with different curing times. (*a*) 4, (*b*) 5, (*c*) 10 and (*d*) 30 min. For curing times greater than 30 min, no further changes are observed. The dimensions of the regions shown are $14{\cdot}4 \times 17{\cdot}2\,\mu\mathrm{m}^2$.

find that when the average void size becomes smaller than approximately 0·4–0·5 μm a transition from two- to one-stage switching is observed. Also, it is noteworthy that it is not until the later stages of polymerization [figure 13 (*d*)] that the helical order within the polymer network is readily observable with SEM.

4. Conclusions

We have studied the effect of UV curing conditions on the electro-optical and morphological properties of 6 wt % RM206 PSCT cells. In general, lower curing intensities and longer curing times result in polymer networks characterized by smaller average mesh sizes. However, variation in curing intensity over the range studied (0·05–5·4 $\mathrm{mW\,cm^{-2}}$) has no significant impact on the morphology of the individual polymer strands. As the curing time is increased for fixed UV intensity, the stages of polymerization are readily observable—a low density network which includes plate and bead-like structures is shown to evolve into a dense, highly interconnected network of fine strands.

The transition from one- to two-stage switching in 6 wt % RM206 PSCT cells as the curing intensity is increased and curing time is decreased is consistent with our previously discussed model [4]. Higher curing intensities and shorter curing times both result in polymer networks with larger voids. This, in turn, results in large regions of liquid crystal which are only slightly influenced by the network, thus accounting for two-stage switching, low threshold voltages and long decay times. Either decreasing the curing intensity or increasing the curing time results in the formation of polymer network structures with smaller average mesh sizes in which a single-process reorientation is observed, as well as higher threshold voltages and faster decay times. This follows from the fact that in all regions the liquid crystal material is strongly dominated by the polymer network.

References

[1] Dierking, I., Kosbar, L. L., Lowe, A. C., and Held, G. A., *Liq. Cryst.*, **24** (3).

[2] Broer, D. J., Gossink, R. G., and Hikmet, R. A. M., 1990, *Angew. makromol. Chem.*, **183,** 45; Hikmet, R. A. M., and Zwerver, B. H., 1991, *Mol. Cryst. liq. Cryst.*, **200,** 197; Hikmet, R. A. M., and Zwerver, B. H., 1992, *Liq. Cryst.*, **12,** 319; Hikmet, R. A. M., and Zwerver, B. H., 1993, *Liq. Cryst.*, **13,** 561; Hikmet, R. A. M., 1996, *Liquid Crystals in Complex Geometries*, edited by G. P. Crawford and S. Žumer (London: Taylor & Francis), Chap. 3.

[3] Yang, D.-K., Chien, L.-C., and Doane, J. W., 1992, *Appl. Phys. Lett.*, **60,** 3102; Yang, D.-K., West, J. L., Chien, L.-C., and Doane, J. W., 1994, *J. appl. Phys.*, **76,** 1331; Yang, D.-K., Chien, L.-C., and Fung, Y. K., 1996, *Liquid Crystals in Complex Geometries*, edited by G. P. Crawford and S. Žumer (London: Taylor & Francis), Chap. 5.

[4] Dierking, I., Kosbar, L. L., Afzali-Ardakani, A., Lowe, A. C., and Held, G. A., 1997, *J. appl. Phys.*, **81,** 3007.

[5] Held, G. A., Kosbar, L. L., Dierking, I., Lowe, A. C., Grinstein, G., Lee, V., and Miller, R. D., 1997, *Phys. Rev. Lett.*, **79,** 3443.

[6] Rajaram, C. V., Hudson, S. D., and Chien, L.-C., 1995, *Chem. Mater.*, **7,** 2300.